Mathematical Modeling of a Solid-State Limiting Current Carbon Monoxide Sensor

Y. Tan and T. C. Tan
Dept. of Chemical Engineering, National University of Singapore, Singapore 0511

A solid-state carbon monoxide sensor was fabricated using a 9% yttria-stabilized zirconia (YSZ) disc sandwiched between two platinum thin-film electrodes. One of the electrodes was coated with a thin layer of 7 $CuO \cdot 10\ ZnO \cdot 3\ Al_2O_3$ catalyst. The sensor showed limiting current behavior at an applied voltage between 0.5 and 1.2 V. Linear response was observed with carbon monoxide in a nitrogen–oxygen mixture at high temperature and limiting current conditions. The linear carbon monoxide concentration range increased with increase in the operating temperature and its sensitivity increased from 2.437 $mA \cdot atm^{-1}$ CO at 1,023 K to 10.771 at 1,093 K. These characteristics were adequately described by the proposed mathematical model relating the response to the rate processes occurring in the catalyst layer and in the electrochemical cell under limiting current conditions. The model showed that effective sensing and high sensitivity are best obtained using a catalyst with high catalytic activity toward the test solute and proper design and fabrication of the sensor to ensure its high diffusivity in the catalyst.

Introduction

In recent years, the increasing global awareness that the world shares a common atmosphere has instilled substantial international concern and instigated increasing cooperative effort to control its pollution, in particular pollutants from the chemical, petrochemical, petroleum refining, metallurgical and industrial combustion processes, and vehicular emission. *In situ* measurement and monitoring of these gas pollutants are indispensable activities of these environmental control programs. Since Kiukkola and Wagner (1957) first described the ionic transport property of solid electrolyte and Weissbart and Ruka (1961) reported their oxygen sensor using yttria-stabilized zirconia (YSZ) solid electrolyte, solid electrolyte electrochemical gas sensors have been increasingly used for high-temperature gas monitoring (Tan and Tan, 1992). Among these, the solid-state Pt/YSZ/Pt oxygen sensor is perhaps most successfully commercialized (Kimura et al., 1986; Maskell and Steele, 1986; Takeuchi and Igarashi, 1988a; Logothetis, 1991; Möbius, 1991). In the potentiometric mode, the platinum electrodes are exposed separately to a reference oxygen mixture and the test sample. The Faradaic reactions described in Eqs. 1 and 2 induce in the cell an emf (E) according to the Nernst equation given in Eq. 3.

$$\text{Cathode:}\quad O_2 + 4e^- \rightarrow 2O^{2-} \tag{1}$$

$$\text{Anode:}\quad 2O^{2-} \rightarrow O_2 + 4e^- \tag{2}$$

$$E = \left[\frac{RT}{4F}\right] \ln\left[\frac{P_{O_2,(\text{sample})}}{P_{O_2,(\text{reference})}}\right]. \tag{3}$$

Since the induced emf depends on the logarithmic concentration difference, the sensitivity of the potentiometric sensor is inherently low. This is further aggravated by operating temperature fluctuations, solid electrolyte aging with prolonged exposure to high temperature, and interferences from other gases in the mixture (Dietz, 1982; Makovos and Liu, 1991). In the amperometric mode, some of these problems can be effectively resolved (Dietz, 1982; Logothetis and Hetrick, 1986; Saji, 1987; Takeuchi and Igarashi, 1988b; Usui et al., 1989; Liaw and Weppner, 1990; Ioannou and Maskell, 1992; Logothetis et al., 1992). In this case, a cell voltage is imposed and the oxygen is virtually transferred or "pumped" from the ca-

Correspondence concerning this article should be addressed to T. C. Tan.

thodic to the anodic side via the Faradaic reactions described in Eqs. 1 and 2. The current varies quantitatively with oxygen concentration in the gas mixture. Apart from being affected by the applied cell voltage, cell resistance, and gas diffusivity, "oxygen pumping" efficiency and sensor sensitivity also depend significantly on the effectiveness of a diffusion barrier in restricting the diffusion of the gas from the bulk to the cathodic surface. Generally good sensing characteristics were obtained under limiting current conditions by imposing an external voltage sufficiently high to maintain a zero oxygen concentration at the cathodic surface. Under these conditions, the rate is controlled by the diffusion of oxygen to the cathodic surface. Good sensing characteristics were also observed by Makovos and Liu (1991) using a cyclic voltammetric technique with their three-electrode oxygen sensor.

Solid-state YSZ oxygen sensor has been used extensively as a primary sensing element for the fabrication of gas sensors for sensing catalytically oxidizable gas solutes. Okamoto et al. (1980) reported good carbon monoxide sensing characteristics in the temperature range of 533–623 K by covering one of the electrodes of their potentiometric oxygen sensor with a layer of $H_2PtCl_6/\gamma\text{-}Al_2O_3$ mixture to catalyze the oxidation of carbon monoxide. The induced emf was directly calibrated against carbon monoxide concentration in the bulk mixture. A mathematical model by Li et al. (1993) described adequately the sensing characteristics of their potentiometric CO sensor using CuO/ZnO catalyst. Good hydrogen sensing characteristics and correlation according to their proposed mathematical model were also obtained by Tan and Tan (1994) with their potentiometric hydrogen sensor. Platinum, a commonly used electrode material in oxygen and other gas sensors, is known for its catalytic oxidation activity (Engel and Ertl, 1982) and the oxidation rate increases with increasing reactant concentration. Since the bare platinum electrode is exposed to higher reactant concentration, its oxidation rate will be higher than at the catalyst-covered electrode. This would reduce the oxygen concentration difference between the two platinum electrodes and correspondingly a smaller induced emf. Consequently, the higher the reactant concentration, the lower will be the sensor sensitivity. This would further diminish the inherently low sensitivity of a potentiometric sensor. This article described the experimental study and mathematical modeling of a high-temperature amperometric carbon monoxide sensor. The sensor was fabricated by overlaying the platinum cathode of a 9 mol % yttria-stabilized zirconia oxygen sensor with a thin layer of $7\ CuO \cdot 10\ ZnO \cdot 3\ Al_2O_3$ catalyst and used to measure CO concentration in an oxygen–nitrogen mixture under limiting current conditions. The sensor was calibrated based on the difference between the steady-state sensor currents before and after the introduction of carbon monoxide into the carrier gas. The sensor difference response was correlated against CO concentration according to a proposed mathematical model relating the response to the Faradaic reactions of the primary solid-state limiting current oxygen sensor and the various rate phenomena occurring in the catalyst layer.

Experimental

Figure 1 shows the design of the carbon monoxide sensor. The platinum electrodes were printed on the opposite faces

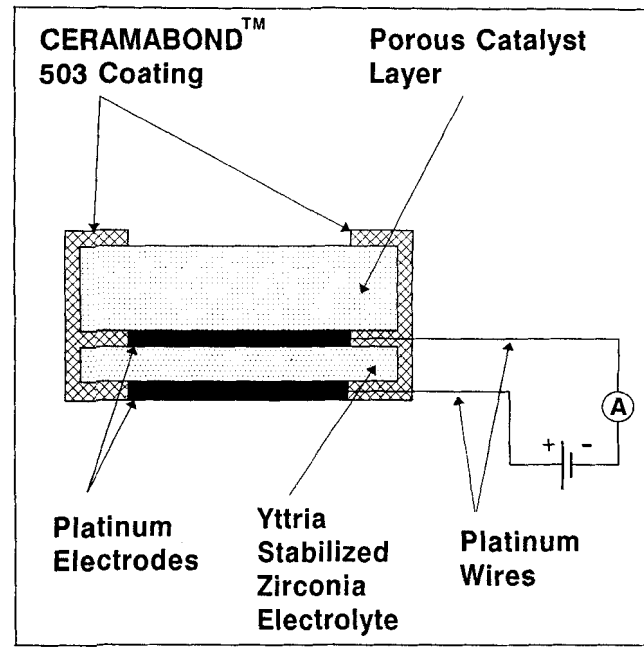

Figure 1. Structural configuration of the carbon monoxide sensor.

of a 9 mol % yttria-stabilized zirconia disc. One of the platinum electrodes was covered by a layer of catalyst while the other was left bare. All the chemicals used were analytical grade.

Pt/YSZ/Pt cell fabrication

The YSZ disc used in fabricating the carbon monoxide sensor was prepared by coprecipitation of the two oxides from a solution of their soluble salts. Subbarao and Maiti (1984) reported that 9 mol % yttria-stabilized zirconia sintered at 1,623 K gave good ionic conductivity and durability. In this study, the 9 mol % YSZ powder was prepared from a solution containing 83.48 mol % of zirconia oxychloride [$ZrOCl_2 \cdot 8H_2O$] and 16.52 mol % of yttrium nitrate [$Y(NO_3)_3 \cdot 5H_2O$] in deionized water. The mixed salt solution and a concentrated ammonia hydroxide solution containing 10% by weight of ammonium carbonate [$(NH_4)_2CO_3$] were added slowly and simultaneously into deionized water, two-and-a-half times the volume of the mixed salt solution. The mixture was constantly stirred and maintained at 323 K. Ammonia solution was added at a rate to maintain the mixture at a pH around 8.5–9. The resulting white spongy precipitate was left in the solution for about an hour without agitation. The solid was then filtered and washed with deionized water until the filtrate showed no trace of chloride by the silver nitrate test. The precipitate was freeze-dried using liquid nitrogen and constant evacuation by a vacuum pump for 24 h. The freeze-dried solids were kept at 393 K for 5 h and then finely pulverized and calcined in a furnace at 973 K for 10 h. The calcined powder was repulverized and pressed into discs of 15 mm dia. and 0.5 mm thick under a pressure of 444 MPa in a Carver Model C metallurgical press. The discs were sintered at 1,623 K for about 5 hours. A 10-mm-dia. circular platinum film of about 0.05 mm thick was printed on both faces of the YSZ

YSZ disc using Ferro 4082 platinum paste. They were left to dry in air for about 5 hours. A fine platinum wire was attached to each electrode with the same platinum paste. The assembly was heated at 1,323 K for 2 hours to remove the organic binder and leave behind a uniform platinum film.

Catalyst pellet preparation

$CuO/ZnO/Al_2O_3$ catalyst is commonly used for water–gas generation (Lloyd et al., 1989) and methanol synthesis (Bridger and Spencer, 1989). Cupric oxide shows better high-temperature adsorption for oxygen than for carbon monoxide and has no affinity for carbon dioxide (Golodets, 1983). Zinc oxide has a stabilizing effect on the catalytic activity of cupric oxide and improves its resistance to sulfide poisoning (Spencer, 1989). Aluminium oxide enhances the mechanical strength and structural stability of the solid mixture. Preliminary studies showed that $CuO/ZnO/Al_2O_3$ in the molar ratio of 7:10:3 has good catalytic activity, mechanical strength, and stability. The catalyst powder was also prepared by coprecipitation of the oxides from their salts. Cupric oxide, zinc oxide, and aluminium sulfate in the molar ratio of 7:10:3 were dissolved in 2N nitric acid. The salt solution and a concentrated sodium hydroxide solution were slowly and simultaneously added into deionized water, two-and-a-half times the volume of the salt solution. The mixture was constantly stirred and maintained at 333 K. Its pH was carefully controlled at about 7 by regulating the addition of the alkali. The resulting blue precipitate was left in the solution for about 5 hours without agitation. It was then filtered and washed with deionized water until the filtrate showed no trace of sulfate by the barium nitrate test. The solid was left to dry in air for 24 hours and then in an oven at 393 K for 5 h. The solid was finely pulverized and calcined at 973 K for about 10 h. The calcined powder was repulverized and pressed into discs of 15 mm diameter and 0.59 mm thick under a pressure of 55 MPa in the Carver press. The discs were sintered at 1,223 K for about 24 hours. The lower pressure of 55 MPa and longer sintering time of 24 hours were used to produce discs with more uniform microstructure, lower tendency to crack, and better structural stability.

Sensor fabrication

Figure 1 shows the design of the sensor. The exposed edges of the YSZ disc were carefully coated with a thin layer of high-temperature CERAMABOND 503 (Components and Products Ltd., Essex, England) ceramic adhesive. The catalyst disc was placed over the YSZ and firmly held together while the sides and edges around the composite disc were covered with a layer of the ceramic adhesive. The whole assembly was dried in air for about 4 hours and the ceramic adhesive seal was then thermally cured in a tubular furnace by heating the air-dried composite pellet to the highest temperature used in this study in three stages as recommended by the manufacturer of CERAMABOND. The three stages consisted of (1) heating at a rate of 5 $K \cdot h^{-1}$ to 367 K and kept at 367 K for 2 h; (2) heating at 20 $K \cdot h^{-1}$ to 644 K and kept at 644 K for 2 hours, and finally (3) heating at 50 $K \cdot h^{-1}$ to the maximum temperature required. The CERAMABOND 503 ceramic adhesive was found effective to shield the YSZ from direct contact with the gas mixture except through the platinum electrodes because of its low porosity (less than 1% after curing). Besides, it has lower thermal expansion and higher mechanical strength than the other components of the sensor.

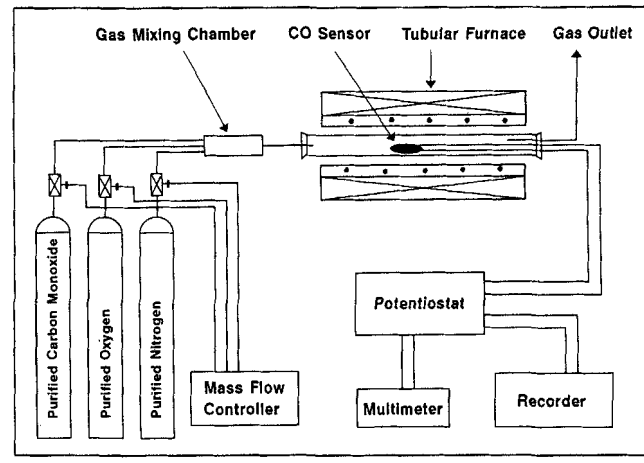

Figure 2. Experimental setup for sensor calibration.

Experimental procedure

The experimental setup is shown in Figure 2. The CO sensor was placed in the middle of the ceramic tube of an Eurotherm tubular furnace. The furnace was gradually heated to a prescribed constant temperature. Compressed purified nitrogen, oxygen, and CO flowed through the respective rotameters into a mixing chamber at ambient temperature (298 K) and pressure. Their flow rates were controlled by an Ultra Mass Flow Controller System (Brooks Model 5850E). The total gas flow rate was maintained at 8.33 $mL \cdot s^{-1}$ for all the experiments. A PINE AFRDE4 potentiostat supplied a constant voltage to the sensor. The sensor current was simultaneously monitored on a chart recorder and a HP 34401A digital multimeter.

Two sets of experiments were carried out at atmospheric pressure. In the first set, the effects of applied cell voltage and oxygen concentration on the sensor current in an oxygen–nitrogen mixture were studied. The oxygen and nitrogen flow rates were varied to give an oxygen partial pressure of 0.01–0.21 atm while maintaining the total flow rate at 8.33 $mL \cdot s^{-1}$. The cell voltage was varied from 0.2 to 1.5 V. In the second set of experiments, the effect of CO concentration on the sensor response was examined at various constant temperatures and at a cell voltage selected from the earlier set of experiments that would effectively maintain the cell at limiting current conditions. In each experiment, the sensor was first exposed to an oxygen–nitrogen mixture of known composition flowing at 8.33 $mL \cdot s^{-1}$. The steady-state current was recorded as the baseline current, I_b. CO was then introduced into the carrier gas at a rate corresponding to a prescribed CO concentration in the mixture. The system was left to equilibrate. When the system reached steady-state, the current, I, was recorded. The sensor response for a given CO concentration was taken as the difference between the two steady-state currents, $(I_b - I)$. The experiment was repeated for other CO concentrations from 0.004 to 0.04 atm at differ-

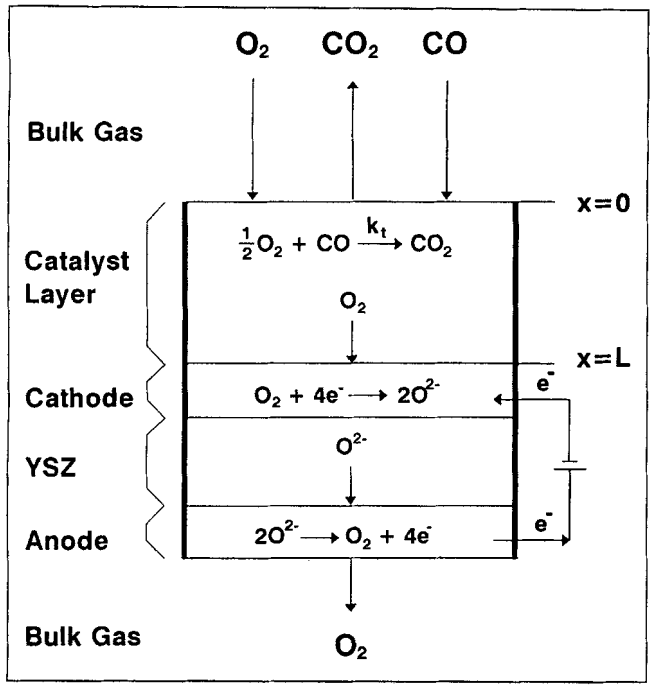

Figure 3. Rate processes occurring in the sensor.

ent constant temperatures from 1,023 to 1,093 K. The oxygen concentration was maintained at 0.04 atm for the whole set of experiments.

Theoretical Model

The objective of this model is to relate quantitatively the sensor current with and without the presence of carbon monoxide in the gas mixture to the rate processes occurring in the catalyst layer and in the solid-state electrochemical cell as shown in Figure 3. The electrochemical cell is assumed to operate under limiting current conditions corresponding to a sufficiently high imposed cell voltage such that the oxygen concentration at the cathode is zero.

Carbon monoxide is oxidized catalytically by the oxygen adsorbed on the catalyst surface (Golodets, 1983; Bielań and Haber, 1991) as shown in Eqs. 4–6:

$$O_2 + s \xrightarrow{k_s} O_2 \cdot s \tag{4}$$

$$O_2 \cdot s + s \xrightarrow[\text{fast}]{k^*} 2O \cdot s \tag{5}$$

$$CO + O \cdot s \xrightarrow{k_{CO}} CO_2 + s, \tag{6}$$

where s is an active site on the catalyst. The overall reaction is given by

$$\frac{1}{2}O_2 + CO \xrightarrow{k_t} CO_2. \tag{7}$$

Assuming homogeneous catalytic activity, the rate equations for the preceding reactions are

$$-r_{O_2} = -\frac{dP_{O_2}}{dt} = k_s \theta_s P_{O_2} \tag{8}$$

$$-r_{CO} = -\frac{dPC_O}{dt} = k_{CO} \theta_O P_{CO} \tag{9}$$

$$r_{\theta_{O_2}} = \frac{d\theta_{O_2}}{dt} = k_s \theta_s P_{O_2} - k^* \theta_{O_2} \theta_s = 0 \tag{10}$$

$$r_{\theta_O} = \frac{d\theta_O}{dt} = 2k^* \theta_{O_2} \theta_s - k_{CO} \theta_O P_{CO} = 0 \tag{11}$$

$$\theta_O + \theta_{O_2} + \theta_s = 1, \tag{12}$$

where θ_s is the fraction of the active sites that are vacant, θ_{O_2} the fraction occupied by the adsorbed molecular oxygen, and θ_O the fraction occupied by the adsorbed atomic oxygen; k_s is the rate constant of the adsorption of O_2 on the catalyst surface; k^* the rate constant for the dissociation of the adsorbed molecular oxygen to its atomic form; and k_{CO} the rate constant for the single-site oxidation of carbon monoxide. The active site distribution is obtained by solving Eqs. 10–12 simultaneously as shown below:

$$\theta_{O_2} = \frac{k_s}{k^*} P_{O_2} \tag{13}$$

$$\theta_s = \frac{k_{CO} P_{CO} (k^* - k_s P_{O_2})}{k^* (2k_2 P_{O_2} + k_{CO} P_{CO})} \tag{14}$$

$$\theta_O = \frac{2k_s P_{O_2} (k^* - k_s P_{O_2})}{k^* (2k_s P_{O_2} + k_{CO} P_{CO})}. \tag{15}$$

Since the sensor is in the form of a thin disc and its edges are coated with a gas-impermeable film, mass transfer will primarily occur in the axial direction and the system is one-dimensional. Assuming $k^* \gg k_s \gg k_{CO}$, the material balance equations for oxygen and carbon monoxide in the catalyst layer are given by

$$D_{O_2} \frac{d^2 P_{O_2}}{dx^2} - \frac{1}{2} k_{CO} P_{CO} = 0 \tag{16}$$

$$D_{CO} \frac{d^2 P_{CO}}{dx^2} - k_{CO} P_{CO} = 0, \tag{17}$$

where D_{O_2}, P_{O_2} and D_{CO}, P_{CO} are the diffusivities and partial pressures of oxygen and carbon monoxide in the catalyst layer, and x the distance from the gas–catalyst interface. Only oxygen ions but not molecular CO can enter and be transported across the YSZ electrolyte to the anode. Under limiting current conditions when oxygen concentration at the catalyst-covered cathode is zero, the boundary conditions are at the gas–catalyst interface:

$$x = 0: \quad P_{O_2} = P_{O_2,b} \quad \text{and} \quad P_{CO} = P_{CO,b}. \tag{18}$$

and at the catalyst–cathode interface:

$$x = L: \quad P_{O_2} = 0, \quad \text{and} \quad \frac{dP_{CO}}{dx} = 0. \tag{19}$$

Equations 20 and 21 which describe the partial pressure profiles of carbon monoxide and oxygen in the catalyst layer, respectively, are derived by solving the material balance Eqs. 16 and 17.

$$P_{CO} = P_{CO,b}\left[\frac{\cosh\left\{mL\left(1-\frac{x}{L}\right)\right\}}{\cosh mL}\right] \tag{20}$$

$$P_{O_2} = P_{O_2,b}\left[1-\frac{x}{L}\right] - \frac{D_{CO}P_{CO,b}}{2D_{O_2}}\left\{1-\frac{x}{L} + \left[\frac{x}{L}-\cosh\left\{mL\left(1-\frac{x}{L}\right)\right\}\right]\operatorname{sech} mL\right\} \tag{21}$$

where

$$m = \sqrt{\frac{k_{CO}}{D_{CO}}}. \tag{22}$$

The limiting current I(mA) depends on the oxygen concentration gradient at the catalyst–cathode interface ($x = L$) and is given by Eq. 23:

$$I(mA) = -\frac{4FAD_{O_2}\times 10^3}{RT}\left[\frac{dP_{O_2}}{dx}\right]_{x=L} \tag{23}$$

where A is the electrode area, F the Faraday constant, and R the gas constant. Combining with the oxygen concentration profile given in Eq. 21, Eq. 24 showing the effect of bulk composition of the gas mixture on the limiting current, I, can be derived:

$$I(mA) = \frac{4\times 10^3 FAD_{O_2}}{RTL}\left[P_{O_2,b} - \frac{D_{CO}P_{CO,b}}{2D_{O_2}}(1-\operatorname{sech} mL)\right]. \tag{24}$$

The baseline current, I_b, at $P_{CO,b} = 0$ and $P_{O_2,b}$ is then given by

$$I_b(mA) = \frac{4\times 10^3 FAD_{O_2}}{RTL} = P_{O_2,b} \tag{25}$$

and the sensor response, $(I_b - I)$ becomes

$$\Delta I(mA) = I_b - I = \left[\frac{2\times 10^3 FAD_{CO}(1-\operatorname{sech} mL)}{RTL}\right]P_{CO,b}. \tag{26}$$

The temperature effect on the diffusivity of CO (D_{CO}) and the surface reaction rate constant (k_{CO}) can be described by the Arrhenius equation:

$$D_{CO} = D^{\circ}_{CO}\exp\left[-\frac{E_{D(CO)}}{RT}\right] \tag{27}$$

$$k_{CO} = k^{\circ}_{CO}\exp\left[-\frac{E_{k(CO)}}{RT}\right]. \tag{28}$$

These are incorporated into the sensor response equation to give Eq. 29, which can be used to correlate the experimental response data:

$$\Delta I(mA) = \frac{2{,}000FA}{RTL}D^{\circ}_{CO}\exp\left(-\frac{E_{D(CO)}}{RT}\right) \times\left[1-\operatorname{sech}\left\{L\sqrt{\frac{k^{\circ}_{CO}}{D^{\circ}_{CO}}}\exp\frac{E_{D(CO)}-E_{k(CO)}}{2RT}\right\}\right]P_{CO,b}. \tag{29}$$

Results and Discussion

Oxygen-sensing characteristics

All the experiments were carried out at atmospheric pressure with a nitrogen–oxygen mixture of known compositions. Preliminary experiments showed that increasing the total flow rate from 3.33 to 5 mL·s^{-1} increased the current response by only about 1.7% and no further change was observed at above 5 mL·s^{-1}. Hence to ensure negligible mass-transfer resistance in the bulk gas mixture, all the experiments were carried out at a total gas flow rate of 8.33 mL·s^{-1}. Figure 4 shows the effect of applied voltage and oxygen concentration

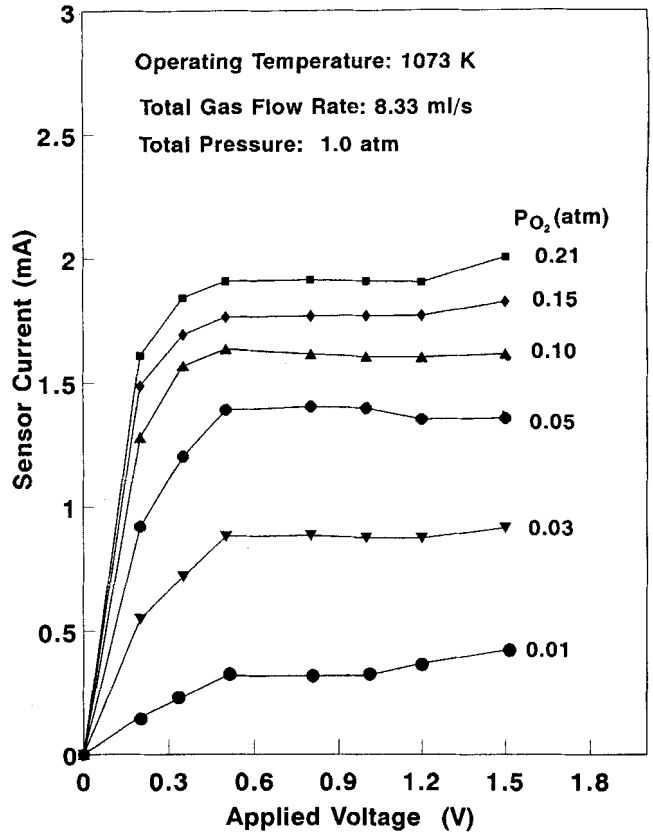

Figure 4. Effect of applied voltage on the sensor current at various constant oxygen concentrations.

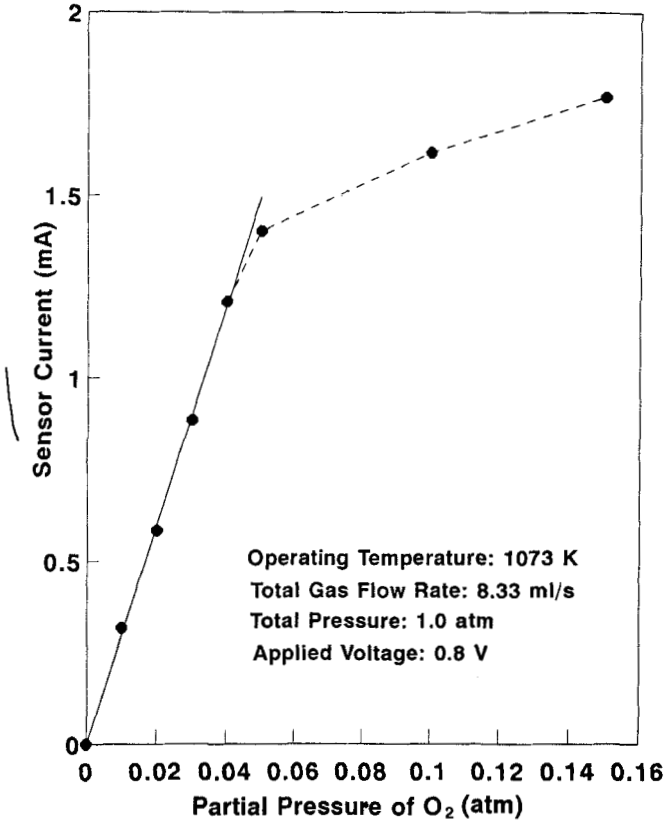

Figure 5. Effect of oxygen concentration on the sensor current at 1,073 K and an applied voltage of 0.8 V.

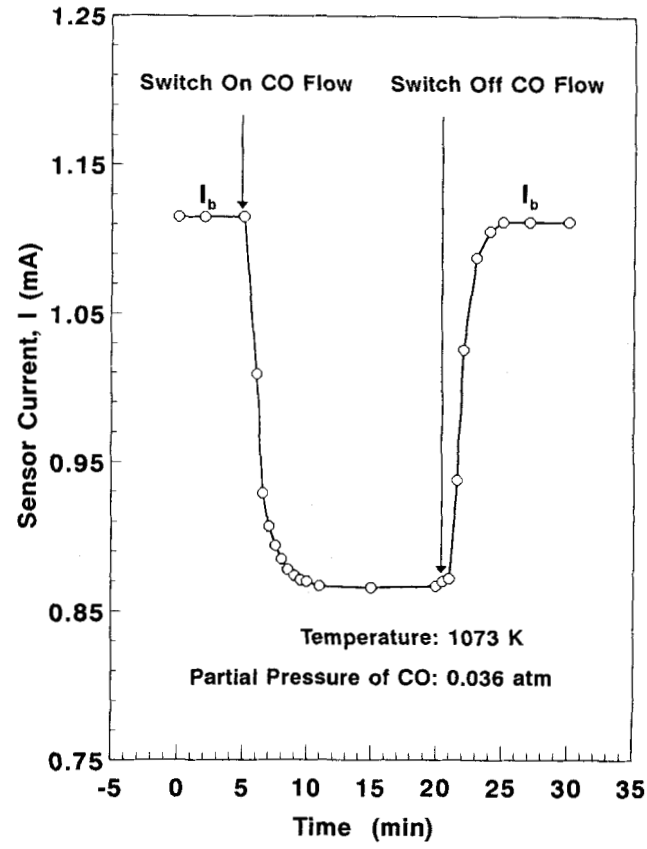

Figure 6. Typical sensor behavior at 0.8 V toward the presence of carbon monoxide in the gas mixture.

on the sensor response at 1,073 K. The sensor current increased with increasing oxygen concentration. At any constant oxygen concentration, the current increased sharply as an external voltage was imposed. It then settled fairly rapidly to a constant value as the voltage increased to above 0.5 V and remained constant until about 1.2 V. The rate of increase and the limiting current values were higher at oxygen concentration. These results showed that the sensor current depends significantly on the mass transfer of oxygen from the bulk to the cathode through the catalyst layer and the cathodic reduction of oxygen. Both these rate processes increased with increasing oxygen concentration and cell voltage. Limiting current conditions indicate a zero oxygen concentration at the cathode and a diffusion controlled system. Under these conditions, maximum sensor current and good stability were obtained. Figure 5 shows the effect of oxygen concentration on the sensor current under limiting current conditions at 0.8 V. The response increased linearly until an oxygen partial pressure of about 0.05 atm, and then more gradually with further concentration increase. The deviation from linearity at high oxygen concentrations could be due to a transition from the diffusion-controlled regime into a regime where the mass-transfer rates became comparable with the Faradaic reactions at the electrodes.

Carbon monoxide sensing characteristics

The results obtained earlier showed that a cell voltage of 0.5–1.2 V is required to maintain limiting current conditions in a bulk gas with an oxygen partial pressure as high as 0.21 atm. All experiments with carbon monoxide were therefore carried out at an imposed cell voltage of 0.8 V using a nitrogen–oxygen carrier gas containing 0.04 atm of oxygen and at a total flow rate of 8.33 $mL \cdot s^{-1}$ at atmospheric pressure. Figure 6 shows the response of the sensor at 1,073 K when CO was introduced into the carrier gas to give a CO partial pressure of 0.036 atm. The current decreased instantaneously and reached a constant value 5 minutes after CO was admitted into the system. About 80% of the current drop occurred in the first 30 s. When the flow of CO was cut off, the current increased instantaneously and reached its original value in about 3 minutes. Sixty-five percent recovery occurred in the first 30 s. Measurement was repeated for other concentrations of CO and temperatures. The baseline current varied slightly between measurements, but the difference between two steady-state values, $(I_b - I)$, remained substantially constant and reproducible. This is a salient advantage of using the difference response method since the prevailing conditions during any single measurement would equally affect both the steady-state sensor currents. Figure 7 shows the calibration plots for different CO concentrations and at different temperatures. The linear range increased with operating temperature, and the maximum CO concentration varied from 0.02 atm or 2 mol % at 1,023 K to 0.04 atm or 4 mol % at 1,093 K.

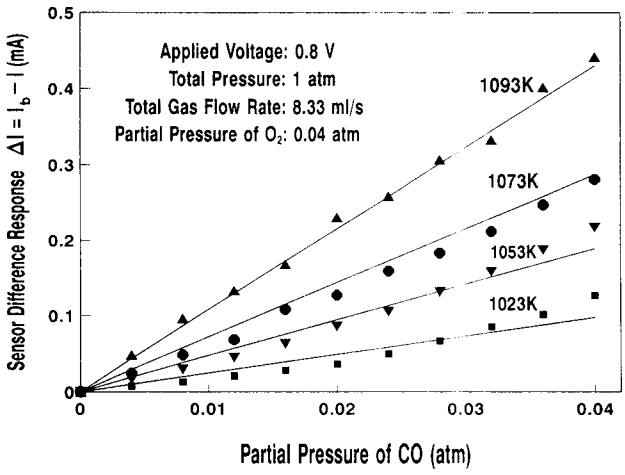

Figure 7. Effect of concentration of carbon monoxide on the difference response of the sensor at various constant temperatures in an oxygen–nitrogen mixture containing 4 mol % oxygen.

Symbols represent experimental values and solid lines are computed from correlation with the model.

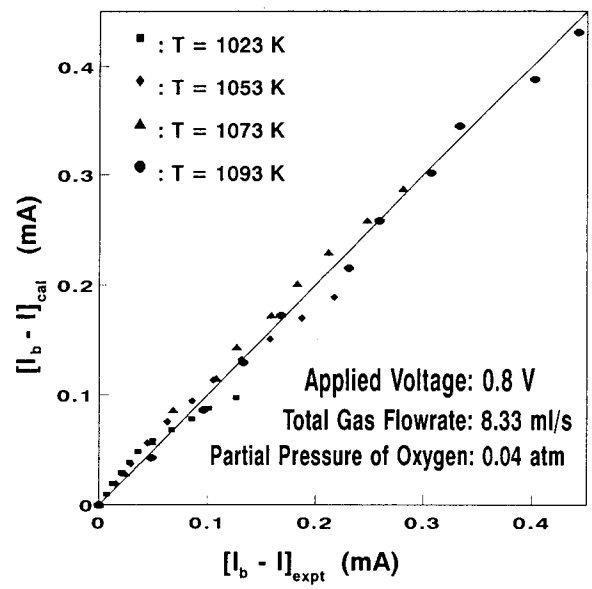

Figure 8. Experimental concentration of carbon monoxide vs. those calculated from the correlation according to the proposed model.

Model verification and correlations of experimental data

The 44 experimental data shown in Figure 7 were correlated together according to Eq. 29. The nonlinear regression involved the evaluation of the frequency factors and activation energies for the diffusion and catalytic reaction of CO in the catalyst layer. The results are given by Eqs. 30–32.

$$D_{CO}(m^2 s^{-1}) = 267.3 \exp\left[-\frac{206{,}140}{RT}\right] \tag{30}$$

$$k_{CO}(s^{-1}) = 4.686 \times 10^5 \exp\left[-\frac{71{,}846}{RT}\right] \tag{31}$$

$$\Delta I(mA) = \frac{8.367 \times 10^{13}}{T} \exp\left[-\frac{24{,}794}{T}\right] \times \left[1 - \text{sech}\left\{0.0247 \exp\left(\frac{67{,}147}{T}\right)\right\}\right] P_{CO,b}, \tag{32}$$

where $P_{CO,b}$ is the partial pressure (atm) of carbon monoxide in the bulk gas mixture. The results computed from Eq. 32 for each of the operating temperatures are plotted as solid lines in Figure 7. Over the temperature range of 1,023 K–1,093 K, the diffusivity of CO through the catalyst layer varied from 7.967×10^{-9} to 3.762×10^{-8} $m^2 \cdot s^{-1}$ with an activation energy of 206.1 $kJ \cdot mol^{-1}$. These are within the range of values given by Barrer (1951) for gas diffusion in porous materials. The reaction constant for the catalytic oxidation of CO varied from 101.1 to 173.6 s^{-1} with an activation energy of 71.8 $kJ \cdot mol^{-1}$. An activation energy of 38 $kJ \cdot mol^{-1}$ was reported for the catalytic oxidation of CO by CuO at 543 K–728 K and ZnO at 693 K and that the values would be higher at higher temperature (Golodets, 1983). This is consistent with the higher values obtained in this study. Both the diffusivities of the gas reactants and the reaction constant of the catalytic oxidation in the catalyst also depend significantly on the characteristics of the porous catalyst disc such as porosity, pore size and pore-size distribution, surface area, and active site density. Equation 32 gives a mean ratio of $\Delta I(\text{cal})/\Delta I(\text{exp})$ of 1.084 with a standard deviation of 0.17 and a mean absolute fractional error of 0.113 with a standard deviation of 0.097. Figure 8 shows the plot of calculated sensor response against the experimental values for all the data shown in Figure 7. The sensor response characteristics are therefore well described by the model, particularly at high temperatures and for CO partial pressure less than 0.025 atm at low temperatures.

The value of the "sech" term in Eq. 32 is negligibly small (10^{-18}–10^{-29}) because of the vast difference in the values between the catalytic reaction rate constant and the diffusivity of CO in the catalyst layer. The design equation for the sensor is therefore reduced to

$$\Delta I(mA) = \frac{8.367 \times 10^{13}}{T} \exp\left[-\frac{24{,}794}{T}\right] P_{CO,b}. \tag{33}$$

This showed that the sensor response for CO is controlled effectively by the diffusion of the carbon monoxide in the catalyst layer. These results suggest that under limiting current conditions, sensing effectiveness and sensitivity of the sensor are best obtained with a catalyst showing high catalytic activity for the test solute and a proper sensor design and fabrication method to ensure high diffusivity of the solute in the catalyst layer.

Conclusions

A solid-state limiting current carbon monoxide sensor was fabricated by overlaying the platinum cathode of a Pt/YSZ/Pt electrochemical cell with a thin compact layer of $7CuO \cdot 10ZnO \cdot 3Al_2O_3$ catalyst. Both the 9% YSZ solid elec-

trolyte and the mixed oxide catalyst were prepared by coprecipitation of the oxides from their soluble salts. Response stability and sensitivity were best obtained under diffusion-controlled or limiting current conditions. Limiting current conditions were obtained under a cell voltage of 0.5–1.2 V for an oxygen partial pressure up to 0.21 atm. Operating at 0.8 V and at constant temperature between 1,023 and 1,093 K, the sensor was calibrated up to a maximum CO concentration of 0.04 atm in an oxygen–nitrogen carrier gas containing 0.04 atm of oxygen. The sensor response toward CO was taken as the difference between the two steady-state sensor currents with and without the carbon monoxide in the feed gas. Linear response was observed and adequately described by a proposed mathematical model relating the response to the rate phenomena occurring in the catalyst layer and the electrochemical cell under limiting current conditions. The CO sensitivity increased from 2.437 $mA \cdot atm^{-1}$ CO at 1,023 K to 10.771 at 1,093 K. The model showed that for the catalyst used, the reaction rate constant was significantly larger than the diffusivity of carbon monoxide in the catalyst layer and the response was effectively controlled by CO diffusion in the catalyst layer. This suggests that high efficacy and sensitivity gas sensors are best obtained using a catalyst with very high catalytic activity for the test solute and a design and fabrication method that would ensure optimum diffusivity of the test solute in the catalyst layer.

Acknowledgments

Research funding by the National University of Singapore and the award of a research scholarship to Y. Tan are gratefully acknowledged.

Notation

d = diameter of the cathode, m
D^{o}_{CO} = frequency factor, diffusivity of carbon monoxide, $m^2 \cdot s^{-1}$
$E_{D(CO)}$ = activation energy, diffusion of carbon monoxide, $J \cdot mol^{-1}$
$E_{K(CO)}$ = activation energy, carbon monoxide catalytic oxidation, $J \cdot mol^{-1}$
ΔI = steady-state difference response of the sensor, $(I_b - I)$, mA
k^{o}_{CO} = frequency factor, catalytic oxidation, s^{-1}
k_l = overall rate constant, s^{-1}
L = thickness of the catalyst layer, m
m = reaction-diffusion parameter defined in Eq. 22, m^{-2}
$P_{O_2,b}$ = partial pressure of oxygen in bulk gas mixture, atm
T = temperature, K

Literature Cited

Barrer, R. M., *Diffusion in and through Solid*, Cambridge Univ. Press, Cambridge, England, p. 91 (1951).
Bielań, A., and J. Haber, *Oxygen in Catalysis*, Marcel Dekker, New York, p. 181 (1991).
Bridger, G. W., and M. S. Spencer, "Methanol Synthesis," *Catalyst Handbook*, M. V. Twigg, ed., Wolfe, England, p. 441 (1989).
Dietz, H., "Gas-Diffusion-Controlled Solid-Electrolyte Oxygen Sensors," *Solid State Ionics*, **6**, 175 (1982).
Engel, T., and G. Ertl, "Oxidation of Carbon Monoxide," *Fundamental Studies of Heterogeneous Catalysis. The Chemical Physics of Solid Surfaces and Heterogeneous Catalysis*, Vol. 4, D. A. King and D. P. Woodruff, eds., Elsevier, Amsterdam, p. 73 (1982).
Golodets, G. I., *Heterogeneous Catalytic Reactions Involving Molecular Oxygen*, Elsevier, New York, p. 284 (1983).
Ioannou, A. S., and W. C. Maskell, "Characterisation of Amperometric Zirconia Oxygen Sensors Prepared Using Planar Thick Film Technology," *Solid State Ionics*, **53/56**, 85 (1992).
Kimura, S., S. Ishitani, and H. Takao, "Principles and Development of a Thick-Film Zirconium Oxide Oxygen Sensor," *Fundamentals and Applications of Chemical Sensors*, D. Schuelzle and R. Hammerle, eds., ACS Symp. Ser. 309, p. 101 (1986).
Kiukkola, K., and C. Wagner, "Measurements on Galvanic Cells Involving Solid Electrolytes," *J. Electrochem. Soc.*, **104**, 379 (1957).
Li, N., T. C. Tan, and H. C. Zeng, "High-Temperature Carbon Monoxide Potentiometric Sensor," *J. Electrochem. Soc.*, **140**, 1068 (1993).
Liaw, B. Y., and W. Weppner, "Low Temperature Limiting Current Oxygen Sensors Using Tetragonal Zirconia as Solid Electrolyte," *Solid State Ionics*, **40/41**, 428 (1990).
Lloyd, L., D. E. Ridler, and M. V. Twigg, "The Water-Gas Shift Reaction," *Catalyst Handbook*, M. V. Twigg, ed., Wolfe, England, p. 283 (1989).
Logothetis, E. M., and R. E. Hetrick, "High-Temperature Oxygen Sensors Based on Electrochemical Oxygen Pumping," *Fundamentals and Applications of Chemical Sensors*, D. Schuelzle and R. Hammerle, eds., ACS Symp. Ser. 309, p. 101 (1986).
Logothetis, E. M., "Automotive Oxygen Sensors," *Chemical Sensor Technology*, Vol. 3, N. Yamazoe, ed., Kodansha, Tokyo, p. 89 (1991).
Logothetis, E. M., J. H. Visser, R. E. Soltis, and L. Rimai, "Chemical and Physical Sensors Based on Oxygen Pumping with Solid-State Electrochemical Cells," *Sens. Actuators B*, **9**, 183 (1992).
Makovos, E. B., and C. C. Liu, "Development of a Solid Electrolyte Sensor for Oxygen in Hot Gases," *Sens. Actuators B*, **3**, 15 (1991).
Maskell, W. C., and B. C. H. Steele, "Solid State Potentiometric Oxygen Sensors," *J. Appl. Electrochem.*, **16**, 475 (1986).
Möbius, H. H., "Solid-State Electrochemical Potentiometric Sensors for Gas Analysis," *Sensors: A Comprehensive Survey*, Vol. 3, W. Göpel, J. Hesse, and J. N. Zemel, eds., VCH, Weinheim, Germany, p. 1105 (1991).
Okamoto, H., H. Obayashi, and T. Kudo, "Carbon Monoxide Gas Sensor Made of Stabilized Zirconia," *Solid State Ionics*, **1**, 319 (1980).
Saji, K., "Characteristics of Limiting Current-Type Oxygen Sensor," *J. Electrochem. Soc.*, **134**, 2430 (1987).
Spencer, M. S., "Fundamental Principles," *Catalyst Handbook*, M. V. Twigg, ed., Wolfe, England, p. 32 (1989).
Subbarao, E. C., and H. S. Maiti, "Solid Electrolyte with Oxygen Ion Conduction," *Solid State Ionics*, **11**, 317 (1984).
Takeuchi, T., and I. Igarashi, "Use of Zirconia Sensors in the Metallurgical Industries in Japan," *Chemical Sensor Technology*, Vol. 1, T. Seiyama, ed., Kodansha, Tokyo, p. 109 (1988a).
Takeuchi, T., and I. Igarashi, "Limiting Current Type Oxygen Sensor," *Chemical Sensor Technology*, Vol. 1, T. Seiyama, ed., Kodansha, Tokyo, p. 79 (1988b).
Tan, Y., and T. C. Tan, "Gas Sensors: A Review," *Bull. SNIC*, **20**, 101 (1992).
Tan, Y., and T. C. Tan, "Characteristics and Modelling of a Solid State Hydrogen Sensor," *J. Electrochem. Soc.*, **141**, 461 (1994).
Usui, T., A. Asada, M. Nakazawa, and H. Osanai, "Gas Polarographic Oxygen Sensor Using an Oxygen/Zirconia Electrolyte," *J. Electrochem. Soc.*, **136**, 534 (1989).
Weissbart, J., and R. Ruka, "Oxygen Gauge," *Rev. Sci. Instrum.*, **32**, 593 (1961).

Manuscript received Oct. 21, 1994, and revision received Apr. 3, 1995.